

HY-2A Radar Altimeter Ultra Stable Oscillator Drift Estimation using Reconstructive Transponder with its Validation by Multi-mission Cross-Calibration

Junzhi Wan, Wei Guo, Fei Zhao, Caiyun Wang* and Peng Liu

Abstract—The paper presents a method estimating the HY-2A altimeter ultra stable oscillator (USO) drift with a reconstructive transponder. The frequency of the USO of the in-orbit altimeter changes with age, and a bias between the actual frequency and the nominal one exists. The USO bias contributes a portion of the altimeter range drift. The HY-2A altimeter transmits signals at a fixed time interval during calibration, and the actual interval between adjacent altimeter transitions, which is controlled by the USO, is different from the nominal one due to the USO drift. The reconstructive transponder measures the arrival times of the altimeter transmitted signals accurately with the atomic clock. The drift of the USO on-board the HY-2A altimeter can be estimated accurately by using the ranges from the reconstructive transponder and the HY-2A altimeter. The USO drifts of around 40 cm/year are presented. Furthermore, the multi-mission cross-calibration provides preliminary validation of HY-2A altimeter USO drift.

Index Terms—Calibration, radar altimetry, transponders, oscillators, frequency,

I. INTRODUCTION

THE essence of the radar altimeter range measurement is the two-way travel time measurement of an altimeter transmitted pulse, and the calculation of the travel time is implemented by counting clock cycles generated by an onboard ultra stable oscillator (USO). The frequency of the oscillator changes slowly with age, and the USO drift contributes a portion of the radar altimeter range bias. The range bias ΔH introduced by USO drift can be written as

$$\Delta H = H \times \frac{\Delta f}{f_0} \quad (1)$$

where H is the altitude of the altimeter above the Earth surface, Δf is the USO frequency bias, and f_0 is the reference oscillator frequency.

This work is part of research toward a Ph.D. being done at the Chinese Academy of Sciences **Key Laboratory of Microwave and Remote Sensing Technology**, National Space Science Center/Center for Space Science and Applied Research, Chinese Academy of Sciences, and the University of Chinese Academy of Sciences.

J. Wan is with the Chinese Academy of Sciences, **Key Laboratory of Microwave and Remote Sensing Technology**, National Space Science Center/Center for Space Science and Applied Research, Chinese Academy of Sciences, Beijing 100190, China, and also with the University of Chinese Academy of Sciences, Beijing 100049, China (e-mail: wanjz.ac@gmail.com).

W. Guo, C. Wang, F. Zhao and P. Liu are with the CAS **Key Laboratory of Microwave and Remote Sensing Technology**, National Space Science Center/Center for Space Science and Applied Research, Chinese Academy of Sciences, Beijing 100190, China (e-mail: guowei@mirslab.cn; wangcaiyun@mirslab.cn; zhaofei@mirslab.cn; liupeng@mirslab.cn).

*Corresponding author.

There are several advanced approaches including those described in this paper to calibrate the altimeter USO drift. Approach I: Lillibrige *et al.* [1] reprocess Waveform Data Records (WDRs) and Sensor Data Records (SDRs) of the Geodetic Mission (GM) of Geosat and obtain a model of the oscillator drift using the time items of SDRs and WDRs. A range-dilation correction at 1 mm level is claimed to be achieved with this model. In our opinion, it is difficult to use drift calibration by data records reprocessing for operational altimetry services. For example, Jason-1 mission provides Interim Geophysical Data Records (IGDR) with a 3-day latency [2], and OSTM/Jason-2 mission provides IGDR with a 1-day latency [3]. Approach II: Scharroo *et al.* [4] proposed a method to model and corrected the ENVISAT RA-2 altimeter range bias attributed to an anomalous operation of the USO by using both the clock of the Instrument Control Unit (ICU) and the USO which provides the frequency standard for the altimeter. Approach III: For the ERS-1/2, the USO frequency is measured once per week over an specific ground station. The USO frequency is recovered on-ground and compared with an atomic frequency standard, then the USO drift correction is obtained [5]. Approach IV: DORIS (Doppler Orbitography and Radio positioning Integrated in Space) instruments onboard the Jason-1, OSTM/Jason-2 and SARAL/AltiKa altimetry satellites provide 10 MHz frequency references for the Poseidon-2/3 and SARAL/AltiKa altimeters [6], [7], and the actual USO frequency can be derived from DORIS data [8]. The Poseidon altimeter onboard the TOPEX/Poseidon satellite also uses time reference provided by DORIS [9]. Approach V: Time Transfer by Laser Link (T2L2) experimental system onboard Jason-2 provides a novel approach to monitor the DORIS oscillators drift [10], [11]. In our opinion, to employ approaches III, IV and V for calibration of the USO as the space-ground time transferring approaches is preferable. This kind of approach relies on a stable USO onboard the altimeter and an accurate monitoring of the USO evolution performed on ground.

MacDORAN *et al.* [12] proposed an active transponder for the calibration of the TOPEX/Poseidon satellite altimetry mission in 1991, which was later called an Active Transponder for Altimetry Calibration (ATAC). Mathews [13] reported the design, laboratory tests and ground filed tests of the ATAC. Compared with traditional transponder for radar altimeter calibration, which receives the altimeter pulse then retransmits the amplified original pulse, the ATAC reconstructs a pulse and sends it back. The signal reconstruction feature enables

the ATAC to adjust the delay of the response pulse precisely. In the following sections, we suggest that the ATAC type transponder can be called reconstructive transponder, unless otherwise stated.

China's marine dynamic environment satellite HY-2A was successfully launched on August 16, 2011. It's nominal orbit altitude is 971 km. A dual-frequency (Ku and C band) radar altimeter is one of HY-2A's main payloads [14], [15]. HY-2A altimeter is a completely redundant altimeter that provides two parallel independent instruments that share a common antenna to meet instrument life requirement, and each instrument, side A and side B, has its own independent USO. In this case, a reconstructive transponder was developed by our laboratory named the Key Laboratory of Microwave and Remote Sensing Technology (Mirslab), CAS (Chinese Academy of Sciences) for the calibration of the active payloads on HY-2A [16], [17]. From August, 2012, the reconstructive transponder has been put into use in the HY-2A altimeter calibration campaign. Discrepancies between the ground observations and the altimeter observations were observed, and the source of the discrepancies was attributed to the USO drift on-board the HY-2A altimeter (the nominal frequency of the HY-2A altimeter USO is 80MHz).

The USO drift corrections presented in this paper are preliminary. The reconstructive transponder utilizes an atomic rubidium clock to generate accurate time reference. The calibration process consists of 4 steps: 1) the altimeter transmits a signal; 2) the reconstructive transponder receives the signal; 3) the reconstructive transponder transmits a reconstructed response signal; and 4) the altimeter receives the response signal, and also can be considered as a time transferring process, during which the altimeter USO drift is estimated using the altimeter observations and the reconstructive transponder observations. Estimating drift of the USO on-board radar altimeter utilizing the reconstructive transponder has not been publicly reported. In this situation, the method using the reconstructive transponder plays a key role in estimating the HY-2A altimeter USO drift.

During calibration campaign, a HY-2A altimeter range bias drift of 40 cm/year was observed. This drift was considered to be caused by USO drift. Bosch *et al.* provided evidences of HY-2A drift by multi-mission cross-calibration [18]. As rigorously calibrated radar altimetry systems, Jason-1 and OSTM/Jason-2 missions with no mean sea level (MSL) drift are sufficient to perform a preliminary validation of HY-2A range drift [19]. Therefore, the crossover differences between the HY-2A altimeter MSL observations and Jason-1 and OSTM/Jason-2 MSL observations are utilized to verify HY-2A altimeter range bias introduced by USO drift.

Details of the approach by using reconstructive transponder are elaborated in the remaining sections of this paper. Section II gives the formulas of ranges from both the altimeter and the reconstructive transponder, and then explains the approach that simplifies the biases introduced by atmosphere. Section III provides the principle of USO drift estimation. Section IV shows the HY-2A USO drift estimation results and corresponding verifications obtained from multi-mission cross-calibration. Section V summarizes the concluding remarks to

complete this paper.

II. ALTIMETER AND TRANSPONDER OBSERVED RANGES

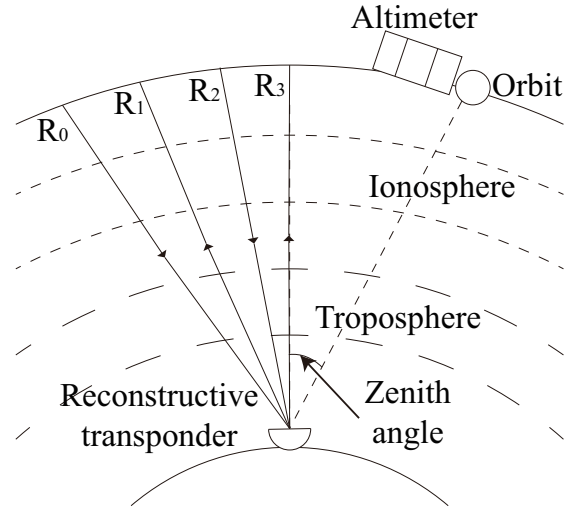


Fig. 1. Geometric relationship between the altimeter and the reconstructive transponder.

Fig.1 shows the geometric relationship between the altimeter and the reconstructive transponder. The HY-2A altimeter is switched to search mode before it overflies the reconstructive transponder. In this mode, the altimeter transmits signals at an interval t_{att} , meanwhile t_{atr} is the interval between a transmission and corresponding receiving operation, and these two intervals are preset constants.

Tropospheric delays, ionospheric delays and instrumental delays exist in the ranges observed by the altimeter and the reconstructive transponder. The instrumental delay of the reconstructive transponder can be taken as a constant D_{tra} , and the instrumental delay of the altimeter introduced by the internal signal path of the altimeter can be taken as a constant D_{alt} (Long term altimeter/transponder path delay change will not affect the final USO frequency estimation, and contents following equation (10) gives the further discussion.). The zenith path delay introduced by the troposphere and the ionosphere can be taken as constants D_{tro} and D_{ion} , and a detailed derivation is contained in appendix. Ground-based global positioning system (GPS) equipment is utilized to obtain the troposphere delay, and total electron content (TEC) global map from International GNSS Service (IGS) is utilized to obtain the ionosphere delay. However, the values of D_{tro} and D_{ion} are not used to obtain the USO frequency (they are used in the further calibration data processing).

Let $R(t)$ be the distance between the altimeter and the reconstructive transponder, and $R(t)$ can be expressed as

$$R(t) = at^2 + bt + c, a \neq 0 \quad (2)$$

where a, b and c are constants [20]. During calibration, Doppler effect introduces bias in the altimeter observations and reconstructive transponder observations. Let $R_k, k = 0, 2, \dots$ be the ranges between the altimeter and the reconstructive transponder when the altimeter transmits the signals, and $R_k, k = 1, 3, \dots$ be the ranges between the altimeter and

the reconstructive transponder when the altimeter receives the response signals. As an example, Fig.1 shows four ranges, R_0 to R_3 . Based on the above discussions of the biases in the observed ranges, let the sum of D_{tra} and D_{alt} is D_{ins} , and the sum of D_{tro} and D_{ion} is D_{atm} , considering the Doppler effect, we get $D_t(k)$, the k th range observed by the reconstructive transponder

$$\begin{aligned} D_t(k) &= (Ct_{att} + R_{2k} + D_{ins} + D_{atm}) \\ &\quad - (R_{2(k-1)} + D_{ins} + D_{atm}) + Dop_{tr} \\ &= Ct_{att} + R_{2k} - R_{2(k-1)} + 2at_{att} \frac{K}{\lambda} \end{aligned} \quad (3)$$

where Dop_{tr} is the Doppler bias, $\lambda = 2.2cm$ is the Ku-Band wavelength of the HY-2A altimeter, C is the speed of light in vacuum and $K = 9.6 \times 10^{-5}$. $R_a(k)$, the k th range observed by the altimeter

$$R_a(k) = R_{2(k-1)} + R_{2k-1} + D_{ins} + 2D_{atm} + Dop_{alt} \quad (4)$$

where Dop_{alt} is the Doppler bias in $R_a(t)$ and $k = 1, 2, \dots$

III. ESTIMATION OF RANGE BIAS DUE TO USO DRIFT

Both the altimeter and the reconstructive transponder are operating by the full deramp principle, therefore, R_{ob} , the ranges observed by the altimeter and the reconstructive transponder, consist of two parts: 1) time-domain range obtained from counting pulses provided by time references (USO on-board the HY-2A altimeter, and atomic clock on-board the reconstructive transponder), 2) frequency-domain range obtained from deramp processing.

The total length of the HY-2A altimeter range window is 60 meters. A 128-points FFT processing divides up the window into 128 range cells, therefore, the frequency-domain one-way range resolution $res_f = 60/128 = 0.46m$. Then we can get

$$RB_{freq} = (FB_{USO}/80MHz) * res_f \quad (5)$$

Where RB_{freq} is the frequency-domain range bias from USO drift, and FB_{USO} is the frequency bias of the HY-2A altimeter USO. Considering the fact that FB_{USO} is no more than $100Hz$, then RB_{freq} is no more than $6 \times 10^{-7}m$. Therefore, RB_{freq} is negligible.

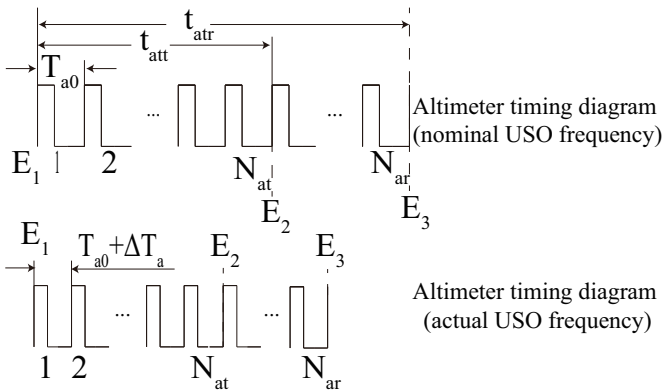


Fig. 2. Altimeter timing diagram with and without USO drift.

Fig.2 shows the altimeter timing diagram with and without USO drift. T_{a0} is the nominal 12.5 nanoseconds period of the

time references of the HY-2A altimeter and the reconstructive transponder, and ΔT_a is the bias of the clock period. t_{att} and t_{atr} are predetermined integer multiples of T_{a0} . The multiples N_{at} and N_{ar} are determined by

$$\begin{aligned} N_{at} &= \frac{t_{att}}{T_{a0}} \\ N_{ar} &= \frac{t_{atr}}{T_{a0}}. \end{aligned} \quad (6)$$

The pulse in Fig.2 is the timing pulse from the altimeter's clock. The altimeter transmits signal Sg_0 at E_1 , the rising edge of the 1st pulse. The echo signal corresponding to Sg_0 is received at E_3 , the rising edge of the $(N_{ar} + 1)th$ pulse. At E_2 , the rising edge of the $(N_{at} + 1)th$ pulse, the altimeter transmits signal Sg_1 . The time interval between E_1 and E_2 is t_{att} , and time interval between E_1 and E_3 is t_{atr} .

N_{at} is uploaded to the HY-2A altimeter before calibration. Considering the existence of ΔT_a and using (6), the Ct_{att} term in (3) becomes $CN_{at}(T_{a0} + \Delta T_a)$, therefore, subtract Ct_{att} from (3), we have

$$\begin{aligned} D(t) &= CN_{at}\Delta T_a + R_{2k} - R_{2(k-1)} + Dop_{tr} \\ &= CN_{at}\Delta T_a + t_{att}(2at' + b) + 2at_{att} \frac{K}{\lambda} \end{aligned} \quad (7)$$

where $t' = t + \frac{t_{atr}}{2}$. According to Fig.1, $R_{2(k-1)}$ and R_{2k} are adjacent ranges that are observed by the reconstructive transponder, and $R_{2k} - R_{2(k-1)}$ is an adjacent range difference term. Therefore, $D(t)$ can be taken as sum of adjacent range difference term, USO range bias $CN_{at}\Delta T_a$, and the Doppler bias. Using (4) and (2), $R_a(t)$, the range observed by the altimeter, can be express as

$$\begin{aligned} R_a(t) &= at^2 + bt + c + a(t + t_{atr})^2 + b(t + t_{atr}) + c + Dop_{alt} \\ &= 2a(t')^2 + (2b + 4a \frac{K}{\lambda})(t') + CN_{at}\Delta T_a + C_1. \end{aligned} \quad (8)$$

where C_1 is a constant. $D(t)$ and $R_a(t)$ are respectively linear function and quadratic function of t' . Therefore, $CN_{at}\Delta T_a$, the range bias introduced by the USO frequency drift of the HY-2A altimeter, can be written as

$$\begin{aligned} CN_{at}\Delta T_a &= \hat{b} - t_{att} \frac{\hat{b}'}{2} \\ &= CN_{at}\Delta T_a + t_{att}b - \frac{2b}{2}t_{att} \end{aligned} \quad (9)$$

where \hat{b} is the constant coefficient of $D(t)$ and \hat{b}' is the linear coefficient of $R_a(t)$, both can be obtained by least square method. The Doppler effects in $D(t)$ and $R_a(t)$ are eliminated, furthermore, D_{ins} and D_{atm} , which are contained in C_1 in (8), do not affect the estimation of ΔT_a .

Δf is the frequency bias of the 80MHz clock that controls the HY-2A altimeter operations, and it can be written as

$$\Delta f = \frac{1}{T_{a0} + \Delta T_a} - f_0 \quad (10)$$

where $f_0 = 1/T_{a0}$ is the nominal frequency of USO. Before using (9), a correspondence between the ranges observed by the altimeter and the reconstructive transponder has to be established, and a matching method introduced by [20] is

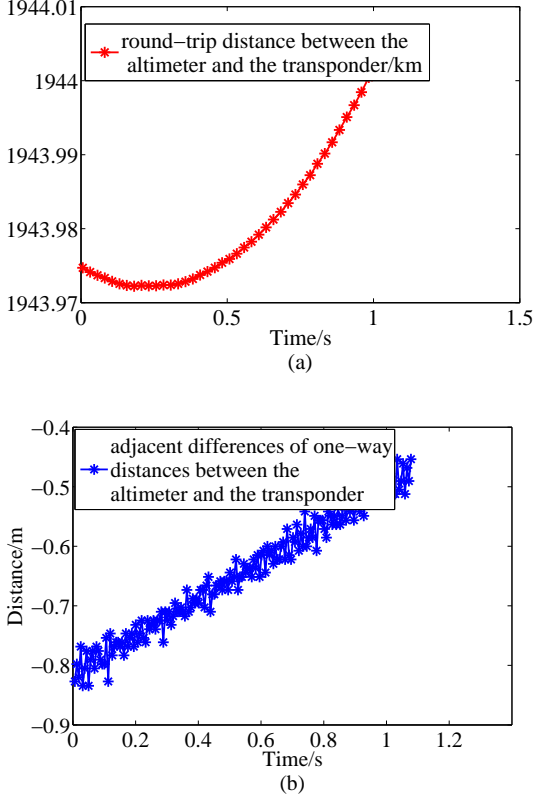


Fig. 3. (a) $R_a(t)$ defined in (8), round-trip distances between the altimeter and the transponder and (b) $D(t)$ defined in (7), adjacent range differences that contain USO range biases and the Doppler biases. HY-2A altimeter records one from each of the four observations during calibration.

utilized.

Fig. 3(a) and Fig. 3(b) show the ranges observed by the HY-2A altimeter and corresponding ranges observed by the reconstructive transponder, which were obtained on September 2, 2012 in Beijing, China. The major portion of HY-2A altimeter's ranges are on the ascending part of the range parabola, therefore, the major portion of the reconstructive transponder's ranges should be positive. However, all of the ranges from the reconstructive transponder are negative because of the bias term $CN_{at}\Delta T_a$ introduced by the HY-2A altimeter USO drift. The level 0 search mode data of the HY-2A altimeter and reconstructive transponder data are used for USO drift estimation. The reconstructive transponder's ranges are produced during calibration, and as soon as the level 0 search mode data of the HY-2A altimeter containing the responding ranges are produced, the range bias introduced by the HY-2A altimeter USO can be estimated and used for range bias correction of the high level data products.

IV. RESULTS, VERIFICATIONS AND DISCUSSIONS

A. HY-2A altimeter USO drift measured by reconstructive transponder

All examples below are from the processing results of the Ku-band data of HY-2A altimeter and the reconstructive transponder, and precision of each parameter, if given, are in the form of 95% confidence bounds unless stated otherwise.

HY-2A USO drift and corresponding range bias observed with the reconstructive transponder are contained in Table I.

An anomalous behavior of HY-2A altimeter side A's USO was reported on March 31, 2013, and side B with an independent USO was brought online on April 2, 2013. From August 9, 2012 to March 2, 2014, a total of 16 USO drift measurements were obtained from HY-2A *in situ* calibrations by using the reconstructive transponder, which are presented in Fig.4, furthermore, corresponding range biases are presented in Fig.4. A piecewise linear character exists in the range bias introduced by the USO of side A except the sample obtained from calibration on March 31, 2013, the same day that anomalous behavior of the USO of the side A was reported, and a single linear trend exists in samples of side B. The slope of each piece is presented. The range bias introduced by the USO can be modeled as

$$\text{range bias} = \begin{cases} 5.36 \times 10^{-4}d + 0.164, & \text{side A : } d \in [359 \ 467] \\ 3.10 \times 10^{-5}d + 0.394, & \text{side A : } d \in [467 \ 579] \\ 1.34 \times 10^{-3}d - 0.697, & \text{side B : } d \in [635 \ 929] \end{cases} \quad (11)$$

where d is the number of days from August 16, 2011.

The USO drifts observed by the reconstructive transponder are not within specifications for the HY-2A altimeter USOs. However, before HY-2A's launching, no abnormal USOs' frequency changes are detected. HY-2A altimeter research group and USO supplier have not yet determined the cause of the USO drift observed by the reconstructive transponder. Both side A and side Bs' USOs frequency increase with age. HY-2A altimeter side A had been working from August 2011 to March 2013, while side B had been at cold standby redundant status, therefore, side A USO's frequency reaches 35Hz and drops, then side B USO is activated, and side B's USO actual frequency starts to increase. Side A USO's voltage anomaly behaviors led to the decision to completely turn off side A, and the relationship between side A USO's frequency drop on March 31, 2013 and the USO's malfunction has yet to be verified. No other abnormal behavior of side B's USO was observed except for large oscillator drift, and it was determined that side B was fit for the HY-2A altimetry mission. HY-2A altimeter USO's drift is larger than most of long-term drifts of the different DORIS on-board oscillators but smaller than Jason's one [21], therefore, such a significant USO shift is not without precedent.

B. USO drift verification by multi-mission cross-calibration

The USO drift in the HY-2A altimeter IGDR products have not been corrected. According to [3], MSL bias of HY-2A altimeter containing USO drift can be expressed as

$$\begin{aligned} \text{MSL Bias} &= \hat{MSL}_{ref} - \hat{MSL}_{HY-2A} \\ &= \text{Bias}_{USO} + \text{Bias}_{others} \end{aligned} \quad (12)$$

where MSL Bias is MSL bias of HY-2A altimeter, \hat{MSL}_{ref} is MSL of a reference radar altimetry mission, \hat{MSL}_{HY} is MSL of HY-2A altimeter, Bias_{USO} is the bias introduced by HY-2A altimeter USO drift, and Bias_{others} is the residual

TABLE I
HY-2A USO DRIFT AND CORRESPONDING RANGE BIAS.

Date/Side	days from August 16, 2011	Frequency bias (Hz)	Range bias (m)
2012-8-9(side A)	359	29.94	0.351
2012-8-19(side A)	369	31.08	0.365
2012-9-2(side A)	383	31.52	0.370
2012-9-6(side A)	387	31.76	0.372
2012-11-15(side A)	457	34.73	0.407
2012-11-25(side A)	467	35.25	0.413
2013-1-20(side A)	523	34.00	0.399
2013-3-3(side A)	565	35.35	0.415
2013-3-17(side A)	579	35.33	0.414
2013-3-31(side A)	593	26.59	0.312
2013-5-12(side B)	635	13.24	0.155
2013-11-24(side B)	831	34.80	0.408
2013-12-8(side B)	845	36.22	0.425
2014-1-5(side B)	873	39.70	0.466
2014-3-2(side B)	929	47.26	0.555

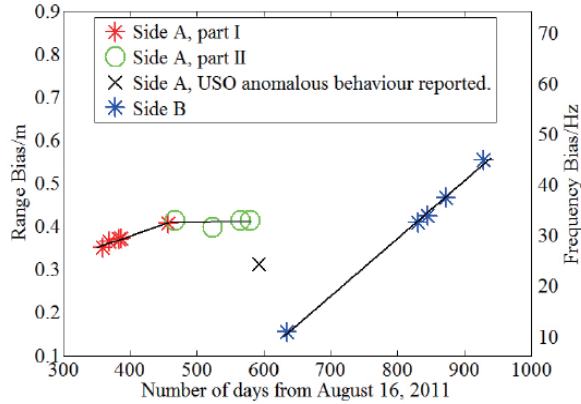


Fig. 4. HY-2A altimeter USO drift and corresponding range bias measured by reconstructive transponder.

bias. We assume that $Bias_{others}$ is a constant term, then the slope of $Bias_{USO}$ equals to the slope of $MSL Bias$. $MSL Bias$ is obtained from cross calibration between the reference radar altimetry mission and HY-2A. 300-second time window and 5-km spatial window are used in cross calibration. Jason-1 and OSTM/Jason-2 mission are used as reference missions.

The USO corrections from the reconstructive transponder are used to correct $MSL Bias$. Jason-1 GDR-C/D data and OSTM/Jason-2 GDR-D data from January 2012 to February 2014 are used to provide reference MSLs. Fig. 5(a) shows the $MSL Bias$ series which utilizes the Jason-1's MSL to make cross calibration with the HY-2A altimeter's MSL, and Fig. 5(b) shows the corrected $MSL Bias$ using (11). The drift of corrected Jason-1-HY-2A $MSL Bias$ is $1.55 \times 10^{-4} \pm$

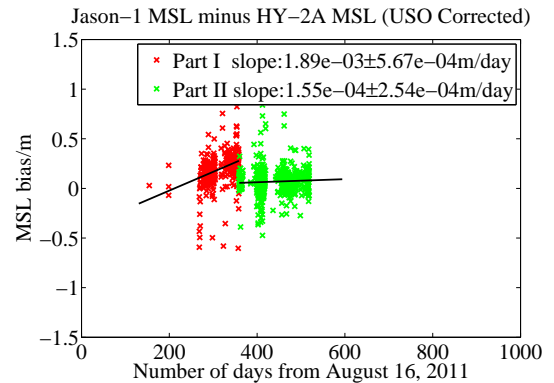
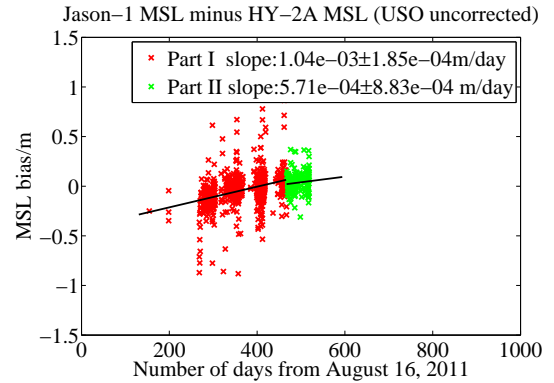


Fig. 5. (a) $MSL Bias$ between Jason-1 and HY-2A. (b) $MSL Bias$ with and without USO bias. Relative biases among pieces are removed. Transponder calibration campaign, as table I shows, starts at day 359 relative to August 16, 2011, and red part of (b) (before day 359) is uncorrected.

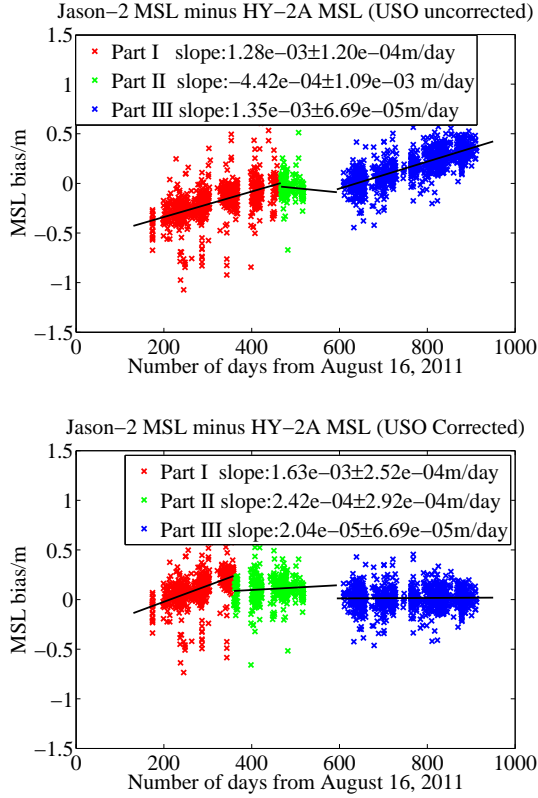


Fig. 6. (a) *MSL Bias* between Jason-2 and HY-2A. (b) *MSL Bias* with and without USO bias. Relative biases among pieces are removed. Transponder calibration campaign, as table I shows, starts at day 359 relative to August 16, 2011, and red part of (b) (before day 359) is uncorrected.

2.54×10^{-4} m/day. Jason-1 mission ended in July 2013, and Jason-1 GDR data corresponding to HY-2A altimeter side-B data are not sufficient to be analyzed. Fig. 6(a) shows the *MSL Bias* series which utilizes the Jason-2's MSL to make cross calibration with the HY-2A altimeter's MSL, and Fig. 6(b) shows the corrected *MSL Bias* using (11). The drift of corrected Jason-2-HY-2A side A *MSL Bias* is $2.42 \times 10^{-4} \pm 2.92 \times 10^{-4}$ m/day, and the drift of side B *MSL Bias* is $2.04 \times 10^{-5} \pm 6.69 \times 10^{-5}$ m/day.

V. CONCLUSION

Though further long term calibration campaign utilizing tide gauge networks is necessary to validate HY-2A altimeter USO drift, due to the 40 cm/year drift of HY-2A altimeter MSL, the reconstructive transponder conducts the USO correction which can guarantee that HY-2A altimeter MSL drift is significantly reduced to 88.3 ± 106.5 mm/year (side A-Jason-2 comparison) and to 7.4 ± 24.4 mm/year (side B-Jason-2 comparison). Up to now, the calibration site of the reconstructive transponder has not been fixed at certain HY-2A crossover yet. Furthermore, several times' complete losses of responding signal occurred due to 1) the uncertainty of orbit prediction in calculating the reconstructive transponder's preset delay, and 2) the limited range window length of HY-2A altimeter in search mode. In order to reduce the losses, we can place the reconstructive transponder at the satellite crossover to upgrade the USO drift estimating accuracy. We have also

suggested that it is preferable to prolong the range window of the following radar altimetry mission in the future to obtain more altimeter observations during transponder calibration. The estimation of the USO drift of the altimeter by using the reconstructive transponder not only provides a novel approach for estimating and calibrating the USO drift of the satellite radar altimeter, but also introduces a method of understanding the oscillator aging characteristic. Besides, the on-board USO drift calibration approach for the following radar altimetry mission to HY-2A has been improved.

ACKNOWLEDGEMENT

This work is supported by 1) CNES AVISO for providing the Jason-1 and OSTM/Jason-2 GDR data, which were produced and distributed by Aviso (<http://www.aviso.altimetry.fr/>), as part of the Ssalto ground processing segment; 2) National Satellite Ocean Application Service (NSOAS) for providing the HY-2A altimeter IGDR and auxiliary data; and 3) Mrs. Li Lan for paper editing.

APPENDIX

TROPOSPHERIC AND IONOSPHERIC DELAYS ANALYSIS

The 3dB beamwidth of the zenith-pointing reconstructive transponder antenna is 1.8 degrees at Ku-band, and the HY-2A altimeter range window is 60 meters wide in search mode. The limited length of HY-2A altimeter range window and the beamwidth of the reconstructive transponder antenna ensure that the angle between the boresight of the reconstructive transponder antenna and the line from the altimeter antenna phase centre to the reconstructive transponder antenna phase centre is no more than 1 degree when the reconstructive transponder signals are in the altimeter range window. The tropospheric delay and ionospheric delay can be approximated by constants under the condition of small angle. The total zenith tropospheric delay is composed of a hydrostatic component, d_{dry} , and a wet component, d_{wet} . The value of d_{dry} is about 2.3 m and relative stable. The value of d_{wet} is small but rapidly changes with time. The tropospheric delay at zenith angle z can be written as

$$D_{tro}(z) = m_d(z)d_{dry} + m_w(z)d_{wet} \quad (13)$$

where $m_d(z)$ and $m_w(z)$ are hydrostatic mapping functions and wet mapping functions, respectively [22]. D_{tro} equals to the total zenith tropospheric delay when $z = 0^\circ$. Niell hydrostatic mapping function and wet mapping function with the same expression [23]

$$m(z) = \frac{1 + \frac{a}{b}}{1 + \frac{c}{a}} \frac{1}{\cos(z) + \frac{b}{\cos(z) + c}} \quad (14)$$

and different a, b, c values in Table II are used in (14) [24]. The ionospheric delay $D_{ion}(z)$ can be written as

$$D_{ion}(z) = d_{iz} \times [1 - (\frac{R_e \sin(z)}{R_e + h_1})^2]^{-\frac{1}{2}} \quad (15)$$

where d_{iz} , R_e and h_1 are zenith ionospheric delay, the Earth's radius and the height of the maximum electron density layer of the ionosphere above the earth's surface [25]. The first order Taylor series expansion of (13) and (15) in the vicinity of $z = 0$ are

$$D_{tro} \approx d_{dry} + d_{wet}, |z| \approx 0 \quad (16)$$

and

$$D_{ion}(z) \approx d_{iz}, |z| \approx 0. \quad (17)$$

a, b, c values in Table II are adopted considering the future alternative *in situ* calibration sites. Suppose $d_{dry} = 2.3m$, $d_{wet} = 0.4m$, $d_{iz} = 0.3m$ (corresponding to Ku-band frequency), $R_e = 6371km$, $h_1 = 350km$, Fig. 7 presents the approximation error when (16) and (17) is used.

TABLE II
VALUES OF TROPOSPHERIC DELAY MAPPING FUNCTION VARIABLES

Parameters		North Latitude	
		15°	45°
Hydrostatic	a	1.2769×10^{-3}	1.2465×10^{-3}
	b	2.9153×10^{-3}	2.9288×10^{-3}
	c	62.6105×10^{-3}	63.7217×10^{-3}
Wet	a	5.8021×10^{-4}	5.8118×10^{-4}
	b	1.4275×10^{-3}	1.4572×10^{-3}
	c	4.3472×10^{-2}	4.3908×10^{-2}

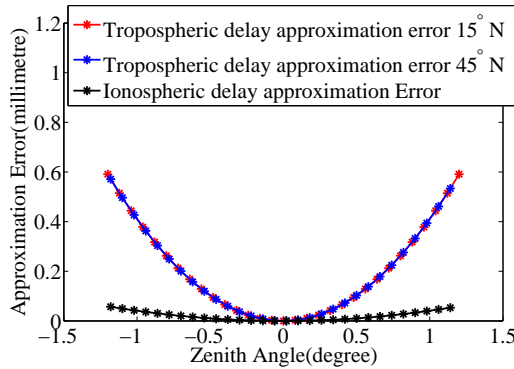


Fig. 7. Tropospheric and ionospheric delays approximation errors.

The total error introduced by the approximations of the tropospheric and ionospheric delays is no more than 1mm at $|z| \leq 1^\circ$, therefore, the zenith path delay introduced by the troposphere and the ionosphere can be taken as constants D_{tro} and D_{ion} .

REFERENCES

[1] J. Lillibridge, W. Smith, R. Scharroo, and D. Sandwell, "The geosat geodetic mission twentieth anniversary edition data product," in *AGU Fall Meeting Abstracts*, vol. 1, 2004, p. 0786.
[2] N. Picot, K. Case, S. Desai, P. Vincent, and E. Bronner, "Aviso and podaac user handbook. igdr and gdr jason products," *SALP-MU-M5-OP-13184-CN(AVISO),JPL D-21352(PODAAC)*, 2012.

[3] J. Dumont, V. Rosmorduc, N. Picot, S. Desai, H. Bonekamp, J. Figa, J. Lillibridge, and R. Scharroo, "OSTM/jason-2 products handbook," *CNES: SALP-MU-M-OP-15815-CN, EUMETSAT: EUM/OPS-JAS/MAN/08/0041, JPL: OSTM-29-1237, NOAA/NESDIS: Polar Series/OSTM J400*, vol. 400, p. 1, 2011.
[4] R. Scharroo, Y. Faugere, P. Féménias, A. Martini, M. Roca, and J. Lillibridge, "Envisat RA-2 USO anomaly: Impact and correction," *ESA Pub. SP*, vol. 636, 2007.
[5] M. Anzenhofer and T. Gruber, "Fully reprocessed ERS-1 altimeter data from 1992 to 1995: Feasibility of the detection of long term sea level change," *Journal of Geophysical Research: Oceans*, vol. 103, no. C4, pp. 8089–8112, 1998.
[6] G. Carayon, N. Steunou, J.-L. Courrire, and P. Thibaut, "Poseidon-2 radar altimeter design and results of in-flight performances special issue: Jason-1 calibration/validation," *Marine Geodesy*, vol. 26, no. 3-4, pp. 159–165, 2003.
[7] P. Vincent, N. Steunou, E. Caubetq, L. Phalippou, L. Rey, E. Thouvenot, and J. Verron, "Altika: a ka-band altimetry payload and system for operational altimetry during the gmes period," *Sensors*, vol. 6, no. 3, pp. 208–234, 2006.
[8] C. Jayles, B. Nhun-Fat, and C. Tourain, "Doris: System description and control of the signal integrity," *Journal of Geodesy*, vol. 80, no. 8-11, pp. 457–472, 2006.
[9] AVISO/Altimetry, *User Handbook for Merged TOPEX/Poseidon products*, 3rd ed. AVISO, 1996, vol. AVI-NT-02-101.
[10] P. Guillemot, K. Gasc, I. Petitbon, E. Samain, P. Vrancken, J. Weick, D. Albanese, F. Para, and J.-M. Torre, "Time transfer by laser link: The t212 experiment on jason 2," in *International Frequency Control Symposium and Exposition, 2006 IEEE*. IEEE, 2006, pp. 771–778.
[11] P. Exertier, E. Samain, C. Courde, N. Martin, J.-M. Torre, J.-L. Oneto, M. Laas-Bourez Geozur, P. Guillemot, and S. Leon, "T212: Five years in space," in *European Frequency and Time Forum International Frequency Control Symposium (EFTF/IFC), 2013 Joint*, July 2013, pp. 632–635.
[12] P. MacDoran and G. Born, "Time, frequency and space geodesy: impact on the study of climate and global change," *Proc. IEEE*, vol. 79, no. 7, pp. 1063–1069, Jul. 1991.
[13] M. B. Mathews, "Design, testing, and performance analysis of transponders for use with satellite altimeters." Ph.D. dissertation, University of Colorado, Boulder, the USA, 1995.
[14] X. Jiang, M. Lin, J. Liu, Y. Zhang, X. Xie, H. Peng, and W. Zhou, "The HY-2 satellite and its preliminary assessment," *International Journal of Digital Earth*, vol. 5, no. 3, pp. 266–281, May. 2012.
[15] K. Xu, J. Jiang, and H. Liu, "HY-2A radar altimeter design and in flight preliminary results," in *Geoscience and Remote Sensing Symposium (IGARSS), 2013 IEEE International*, July 2013, pp. 1680–1683.
[16] W. Guo, X. Y. Gong, X. Y. Xu, H. G. Liu, C. D. Xu, and Y. H. Du, "A transponder system dedicating for the on-orbit calibration of china's new-generation satellite altimeter and scatterometer," in *Radar (Radar), 2011 IEEE CIE International Conference on*, vol. 1, 2011, pp. 22–25.
[17] X. Y. Xu, W. Guo, H. G. Liu, L. W. Shi, W. M. Lin, and Y. H. Du, "Design of the interface of a calibration transponder and an altimeter / scatterometer," in *IEEE IGARSS, 2011*, pp. 953–956.
[18] W. Bosch, D. Dettmering, and C. Schwatke, "Multi-mission cross-calibration of satellite altimeters: Constructing a long-term data record for global and regional sea level change studies," *Remote Sensing*, vol. 6, no. 3, pp. 2255–2281, 2014.
[19] G. P.Prandi, "Validation of altimeter data by comparison with tide gauge measurements," Ref:CLS.DOS/NT/13-285, Tech. Rep., May. 2014.
[20] J. Wan, W. Guo, C. Wang, and F. Zhao, "A matching method for establishing correspondence between satellite radar altimeter data and transponder data generated during calibration," *Geoscience and Remote Sensing Letters, IEEE*, vol. 11, no. 12, pp. 2145–2149, Dec 2014.
[21] J.-M. Lemoine and H. Capdeville, "A corrective model for jason-1 doris doppler data in relation to the south atlantic anomaly," *Journal of Geodesy*, vol. 80, no. 8-11, pp. 507–523, 2006.
[22] E. D. Kaplan and C. J. Hegarty, *Understanding GPS: principles and applications*, 2nd ed. Artech house, 2005.
[23] A. E. Niell, "Global mapping functions for the atmosphere delay at radio wavelengths," *Journal of Geophysical Research: Solid Earth*, vol. 101, no. B2, pp. 3227–3246, 1996.
[24] T. Schuler, *On ground-based GPS tropospheric delay estimation*. Univ. der Bundeswehr München, 2001.
[25] W. MOPS, "Minimum operational performance standards for global positioning system/wide area augmentation system airborne equipment," *RTCA Inc. Documentation No. RTCA/DO-229B*, vol. 6, 1999.



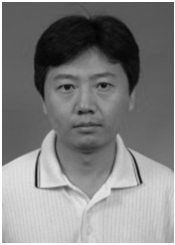
Wan Junzhi received the B.Eng. degree from Huazhong University of Science and Technology, Wuhan, China, in 2010. He is currently working toward the Ph.D. degree in the **Key Laboratory of Microwave and Remote Sensing Technology**, Center for Space Science and Applied Research, Chinese Academy of Sciences, Beijing, China, and the University of Chinese Academy of Sciences, Beijing.

His research interests include data processing and calibration method for microwave remote sensor.



Zhao Fei received the BS degree from Jilin University, Changchun, China, in 2008, the MS degree from University of Chinese Academy of Sciences, Beijing, China, in 2011. He is currently working in **Key Laboratory of Microwave and Remote Sensing Technology**, Chinese Academy of Sciences.

His research interests include development of calibration equipment and calibration algorithm for microwave remote sensor.



Guo Wei received the B.S. degree from Xian Jiaotong University, Xian, China, in 1989, the M.S. degree from Changchun Institute of Geography, Chinese Academy of Sciences (CAS), Changchun, China, in 1994, and the Ph.D. degree from the Institute of Electronics, CAS, Beijing, China, in 1999.

From 1999 to 2001, he did postdoctoral work in sea surface returned signal simulator development for radar altimeter calibration with the Center for Space Science and Applied Research, CAS, Beijing.

He is currently with the **Key Laboratory of Microwave and Remote Sensing Technology**, Center for Space Science and Applied Research, CAS. He became interested in calibration for the HY-2 satellite altimeter by using reconstructive transponder in 2010. His current research interests are microwave remote sensor development and calibration.



Wang Caiyun received the B.Eng. and M.Eng. degrees in communication and information engineering from Xidian University, Xian, China, in 1997 and 2001, respectively. She is an associate professor of the Nation Space Science Center, Chinese Academy of Sciences. Her current research interests include calibration and validation of satellite-borne altimeter, calibration of synthesized aperture radar.



Liu Peng received the Master degree from University of Chinese Academy of Sciences Beijing, China, in 2009. He is currently an assistant professor in the Department of Electronic Engineering, National Space Science Center, Chinese Academy of Sciences, and working toward the Ph.D. degree in the Department of Electronic Engineering. His research interests include high speed digital signal processing and radar altimeter.